

## Silica-protein composite layers of the giant basal spicules from *Monorhaphis*: Basis for their mechanical stability\*

Xiaohong Wang<sup>1,‡</sup>, Ute Schloßmacher<sup>2</sup>, Klaus Peter Jochum<sup>3</sup>,  
Lu Gan<sup>1</sup>, Brigitte Stoll<sup>3</sup>, Iosune Uriz<sup>4</sup>, and Werner E. G. Müller<sup>2,‡</sup>

<sup>1</sup>National Research Center for Geoanalysis, 26 Baiwanzhuang Dajie, CHN-100037 Beijing, China; <sup>2</sup>Institut für Physiologische Chemie, Abteilung Angewandte Molekularbiologie, Universität, Duesbergweg 6, D-55099 Mainz, Germany; <sup>3</sup>Max-Planck-Institut für Chemie, Postfach 3060, D-55020 Mainz, Germany; <sup>4</sup>Department of Aquatic Ecology, Centre d'Estudis Avançats de Blanes, Accés a la Cala St Francesc, 14, ES-17300 Blanes (Girona), Spain

**Abstract:** The hexactinellid sponge *Monorhaphis chuni* possesses with its giant basal spicules the largest biosilica structure on Earth. The approximately 8.5-mm-thick spicules are composed of up to 800 lamellae. By application of high-resolution electron microscopy (HR-SEM), it is shown that within the siliceous lamellae a proteinaceous scaffold exists which is composed of one protein of a size of 27 kDa. Analyses with Fourier transform infrared (FT-IR) emission and energy-dispersive X-ray (EDX) spectroscopy support this localization of the protein. No evidence for the presence of protein on the surfaces of the lamellae could be obtained. Heating the giant basal spicule to 600 °C destroys and eliminates the protein scaffold. At a temperature of 1600 °C, the lamellae fuse to solid glass via a nonstructured, foamed-up molten transition state. Elevation of the temperature to 2700 °C results in the formation of silica drops (*Euplectella aspergillum*). After the elimination of the protein scaffold from the silica lamellae, the spicules lose their mechanical characteristics of the original hydrated silica/protein composite to be flexible and simultaneously stiff and tough. The data presented here are expected to contribute to technologies suited to fabricate novel organic/inorganic (silica) hybrid fibers.

**Keywords:** composite layers; composite materials; *Monorhaphis*; silicate; silicatein; sponges.

### INTRODUCTION

Nature produces the best materials with respect to mechanical, optical, or chemical properties. Therefore, natural bioinorganic materials constitute a rich source of inspiration for novel biomaterials. It was Mayer [1] who categorized and structured the strategies of nature to build rigid materials. Silicon, the second most abundant element on the Earth's crust, forms in combination with oxygen technologically important inorganic compounds [2,3]. Silica ( $\text{SiO}_2 \cdot n\text{H}_2\text{O}$ ) is used as a component for application in opto- and microelectronics; however, the major field of use of biosilica will be expected in the field

\*Paper based on a presentation at the 13<sup>th</sup> International Biotechnology Symposium (IBS 2008): "Biotechnology for the Sustainability of Human Society", 12–17 October 2008, Dalian, China. Other presentations are published in this issue, pp. 1–347.

<sup>‡</sup>Corresponding authors: Tel.: +49-6131-39-25910; Fax: +49-6131-39-25243; E-mail: wmueller@uni-mainz.de (W.E.G. Müller); wxh0408@hotmail.com (X.H. Wang)

of biomedicine and tissue engineering [4,5]. In nature, silica materials are formed by a few uni- and multicellular organisms by processes that offer the prospect of developing environmentally benign routes suitable to synthesize new silicon-based materials [6]. The outstanding feature of one animal phylum, the sponges (Porifera), is that they form silica enzymatically by the enzyme silicatein. This enzyme has been discovered by the group of Morse [7,8] in the siliceous demosponge *Tethya aurantium* and little later found also in other members of that taxon, e.g., *Suberites domuncula* [9]. The kinetics of silicatein follows the characteristic parameters known from other enzymes [10]; it allows the formation of biosilica at ambient temperature and under environmentally safe conditions. It was the group of Mayer [1,11] who recognized that the mechanical stability of the skeletal elements of sponges, the spicules, is based on their unique structure. These spicules are composed of concentrically organized lamellae that provide them with stiffness and simultaneous flexibility through thin organic layers. For the experiments described here, the second class of siliceous sponges, the Hexactinellida, has been used, that offers the advantage to study the properties of their spicules in a clear way. In contrast to those of the Demospongiae, the spicules of the Hexactinellida are usually very large and comprise a morphologically distinct architecture [12,13]. However, the basic structure of the spicules in both classes is identical in that they are constructed by concentrically arranged silica layers [14,15].

Stimulated by the intriguing demonstration that the spicules from both hexactinellids [16] and demosponges [17–19] are built according to strict structural hierarchies, the elucidation of the biochemical and molecular biological basis of the spicule formation started in hexactinellids also. The sponges *Euplectella aspergillum* [1,16] and *Monorhaphis chuni* [20,21] were used as model systems. The giant basal spicules of *M. chuni*, the largest biosilica structure on Earth (length: 3 m; cross-section: 8.5 mm), provided a suitable example for the demonstration of the lamellar organization in hexactinellids. Electron microscopical studies, combined with biochemical investigations, showed that these spicules are composed of 400–800 lamellae that surround the axial filament composed of silicatein. The thickness of an individual lamella is between 4 and 8  $\mu\text{m}$  [20,21]. The major protein species present in these siliceous spicules, the 24/27-kDa polypeptide, cross-reacts with antibodies raised against silicatein [22]. Recently, the gene for silicatein has also been cloned from a hexactinellid [23]. Initially it had been reported that the spicules of *M. chuni* are covered by collagen, while the lamellae contain the 27-kDa protein (likely to be silicatein) and in the core region additionally a protein of higher molecular weight [20–22]. However, a recent study by Ehrlich and colleagues [24] claiming that collagen is present between the lamellae and mediates biosilica formation needs additional investigations; neither protein-biochemical data [sodium dodecyl sulfate-polyacrylamide gel electrophoresis (NaDodSO<sub>4</sub>-PAGE) analysis; 24], nor protein-structural data [matrix-assisted laser desorption/ionization; 25] have been presented.

It is the aim of our study to clarify the location of the proteinaceous material; whether it is located within the lamellae or on the surfaces of the lamellae that compose the giant basal spicules of *Monorhaphis*. Furthermore, the nature of the organic scaffold awaits a further elucidation; for these experiments we used individual lamellae for extraction. By application of high-resolution scanning electron microscopy (HR-SEM), that is flanked by biochemical (NaDodSO<sub>4</sub>-PAGE) and physical techniques [Fourier transform infrared (FT-IR) emission spectroscopy, energy-dispersive X-ray (EDX) spectroscopy] we show that the lamellae contain a 27-kDa protein, likely silicatein, within the silica matrix. After elimination of the organic scaffold by heat, the giant basal spicules lose their characteristic mechanical property, of flexibility with simultaneous stiffness and toughness.

## EXPERIMENTAL PROCEDURES

### Sponges

Spicules (giant basal spicules) from the hexactinellids *M. chuni* (Porifera:Hexactinellida: Amphidiscosida:Monorhaphididae) and *Monorhaphis intermedia* were used as described [20]; Fig. 1.



**Fig. 1** Schematic representation of the hexactinellid sponge *M. chuni*, growing around one giant basal spicule. The animals can reach sizes of up to 3 m and hence form a similarly long giant basal spicule. They represent the largest biosilica structure on Earth. The sessile animals anchor with their giant basal spicule to the substratum of the deep sea. The body is interspersed with ingestion openings allowing a continuous water flow through canals in the interior which open into oscules that are centralized in atrial openings, the sieve-plates.

At present, these two species are considered to be synonymous [26]; therefore, we term this species here operationally *M. chuni*. For the experiments, described here, specimens collected from the South Chinese Sea (Guangzhou Marine Geological Survey; China), have been used.

For the melting experiments, the skeleton of the hexactinellid *Euplectella aspergillum* (Porifera:Hexactinellida:Hexactinosida:Euplectellidae) has been used, since the *Monorhaphis* spicules are too rare for bulk experiments. *E. aspergillum* had been purchased from Cebu City (Cebu; Philippines) and had a size of about 20 cm. In addition, giant spicules from the hexactinellid *Hyalonema sieboldi* (Porifera:Hexactinellida: Amphidiscosida:Hyalonematidae) have been used for the demonstration that during bending of the spicules (length about 300 mm; diameter ~0.8 mm) piles of lamellae are spalling off, starting from the surface of the spicules.

### Spicules and spicule extracts

The spicules were treated with an ultra-sonicator (S3000; IUL Instruments, Königswinter; Germany) to remove loosely attached organic material and then used for the analysis of the collagen sheet attached to their surfaces. In addition, they were treated with sulfuric/nitric acid to assure that all organic material, exposed to the siliceous spicules, had been removed [20].

For the release of the protein lattice the *Monorhaphis* spicules, more precisely their lamellae, were treated with hydrofluoric acid (HF) for 1–5 h as described [7,20,21]. A complete dissolution of

the silica material from the spicules was achieved in a buffered solution of 6 M HF/8 M NH<sub>4</sub>F after 12 h.

For NaDodSO<sub>4</sub>-PAGE analysis, protein from the lamellae from the outer region (1 mm) of the 3–5-mm-thick giant basal spicules was prepared. The lamellae were removed mechanically from the spicules and treated again with sulfuric/nitric acid. Subsequently, the lamellae were subjected to HF until the siliceous material was completely dissolved. Then the suspension was immediately dialyzed (3 times) against 5 l of 50 mM Tris-HCl buffer (pH 9.0; 100 mM NaCl, 10 mM EDTA) at 4 °C for 4 h each. The remaining organic material was collected and analyzed by gel electrophoresis. For the isolation of protein 500 µg of lamellae (starting weight) were extracted with 500 ml of the Tris-HCl buffer. Where indicated, the *Monorhaphis* spicules had been treated in air at 600 °C for 20 min in a tube oven.

### Iridium-strip heater system

The design of the Ir-strip heater has been described in detail [27]. Melting was performed in a sealed steel box under an excess pressure of argon. The spicule samples were placed onto an iridium strip (Heraeus, Hanau; Germany). The strips were clamped onto two copper poles, which were connected to a transformer. The melting time and temperature were set to 5–30 s, and 1600 °C. Temperature measurement was performed with a pyrometer that had been calibrated against a Thermocoax Pt-30 %Rh/Pt-6 %Rh thermal element.

### Melting experiments

For the melting experiments of *E. aspergillum* (drop formation) an acetylene (Linde, Mainz; Germany) flame of a regular workshop burner that generated a temperature of about 2700 °C was used.

### Electron microscopy

HR-SEM analysis was carried out using a broken spicule, lamellae, or the protein material within the lamellae, in a LEO 1530 Gemini field-emission scanning electron microscope (FESEM) within the range 1 and 5 kV. The signals were detected (in-lens annular, secondary electron) and processed (pixel averaging, frame integration/continuous averaging). The samples were mounted onto stubs (carbon adhesive Leit-Tabs G3347 [Plano, Wetzlar; Germany]).

### NaDodSO<sub>4</sub>-PAGE and Western blot analysis

Protein samples from lamellae were subjected to NaDodSO<sub>4</sub>-PAGE. Spicule extracts containing 1–3 µg of protein (equivalent to 50 µg spicular material) were dissolved in loading buffer (Roti-Load; Roth, Karlsruhe; Germany), boiled for 5 min, and then subjected to 10 % PAGE, containing 0.1 % NaDodSO<sub>4</sub> [28]. Details were given earlier [22]. The gels were stained in Coomassie brilliant blue.

Western blot analysis was performed as described [18,22], using polyclonal antibodies that had been raised against silicatein from *S. domuncula* (PoAb-aSilic, No. N365), as described earlier [18].

### Energy-dispersive X-ray analysis

EDX analysis of the spicules was performed on SEM images (back-scattered mode) using a Philips XL 30 ESEM microscope as described [29]. The EDAX Genesis EDX System, attached to a scanning electron microscope (Nova 600 Nanolab; FEI, Eindhoven; The Netherlands) operating at 10 kV with a collection time of 30 s, had been used. Areas of approximately 1–5 µm<sup>2</sup> were analyzed by EDX.

### Fourier transform infrared emission spectroscopy

For FT-IR emission spectroscopy, samples of *Monorhaphis* spicules (3 mg each) were ground in a mortar and milled with potassium bromide (KBr) to a very fine powder. The powder was then compressed into disk pellets. For heat-treated *Monorhaphis* spicules, the cast film technique was applied. The heat-treated spicule (3 mg) was suspended in methylene chloride, placed onto the surface of the KBr disk, and the solvent was evaporated, allowing the spicule to attach to the disk. FT-IR spectra of the heat-treated spicule were recorded on an infrared spectroscope (2030 Galaxy FT-IR spectrometer; Mattson Instruments, Madison, WI, USA) at room temperature as described [30].

### Determination of the mechanical properties of the spicules: Three-point bending system

For the analysis of the flexural properties of the giant basal spicules, specimens between 30 and 35 mm in length were tested as described [26,29,31–33]. The spicules had been stored in wet chambers and kept at 4 °C, prior to use. The thickness of the spicules ranged from 2.1 to 2.5 mm. Samples were cut using a disk saw, to avoid cracking, as described and illustrated [29]. For the determination of the deflection, the spicule sample was fixed in a three-point bending system (WDW 3020, Changchun, China), selecting a fixture with a 20-mm span and an articulated center-loading rod at a cross-head rate of 0.2 mm/min. The measurements were performed with a computer-controlled MTS servo-hydraulic test frame. Both cross-head displacement and load were automatically recorded throughout the tests [29].

### Determination of the mechanical properties of the spicules: Circular bending

A giant spicule from *H. sieboldi* (~300 to ~0.8 mm) had been inserted into a traction device between two moving rubber wheels. Subsequently, a continuous pulling of the spicule was achieved by a motor. The steps of breakage were recorded with a high-speed camera.

### Analytical method

For the quantification of protein, the Bradford method [34] (Roti-Quant solution, Roth) was used.

## RESULTS

The central experiments have been performed with the giant basal spicules from *M. chuni*. For the melting experiments, skeletons of complete specimens of *E. aspergillum* have been used; and for the circumvolution bending experiments, the giant spicules from *H. sieboldi* were employed.

### Proteinaceous component in the lamellae of *M. chuni*

Three different approaches have been applied to demonstrate that the siliceous lamellae (4–7 µm thick) of the spicules contain within their inorganic matrix a proteinaceous scaffold.

#### *Electron microscopic analysis (SEM, HR-SEM)*

As described earlier [29], the surfaces of the spicules, cleaned with sulfuric/nitric acid to remove organic material, and also those of their composing lamellae, are free from detectable organic structures (Fig. 2A), if analyzed by SEM analysis. However, after exposure to HF, the organic scaffold becomes progressively visible. After a short exposure period of 1 h, the decomposition of the silica lamellae starts from the surface of individual lamellae, setting free wrinkled structures (Fig. 2B). A longer exposure period [2 h (Figs. 2C,D) or 5 h (Fig. 2E)] results in a progressive dissolution of the lamellae. After 5 h, the proteinaceous scaffolds within the siliceous matrix of each lamella are uncovered

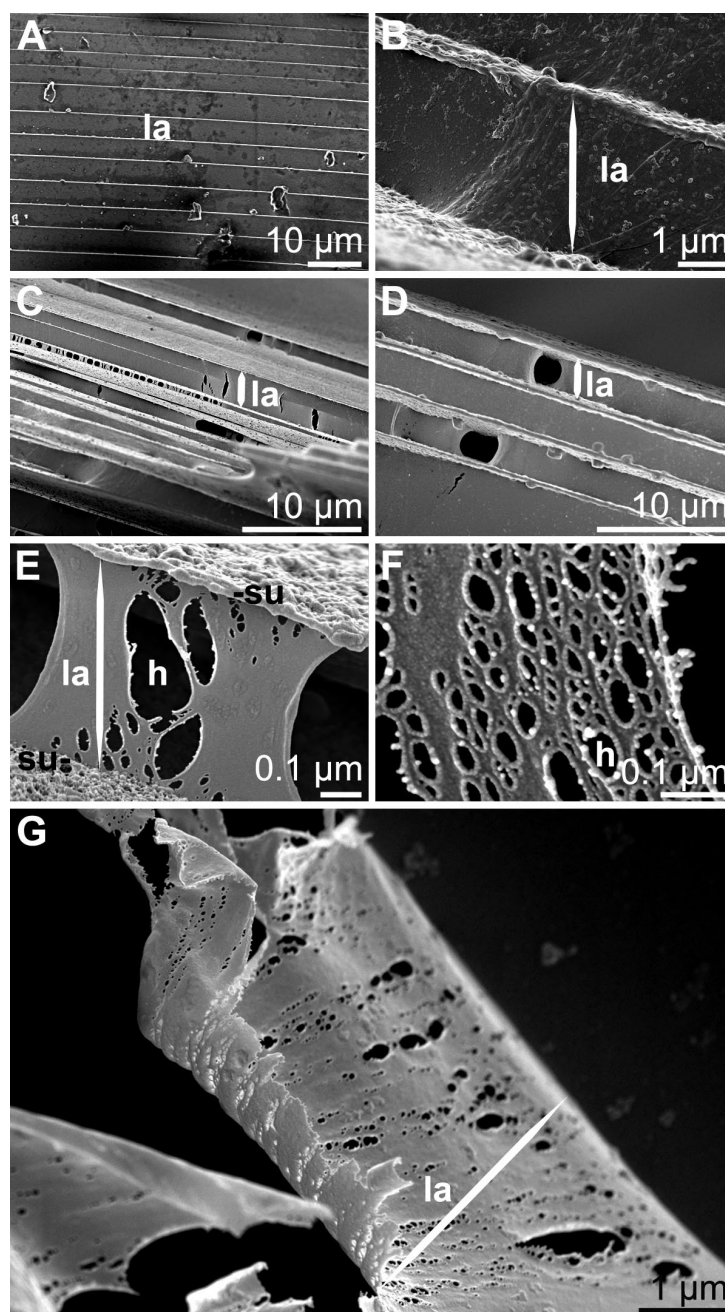


**Fig. 2** HR-SEM analysis of the structure of giant basal spicules in cross breakages. (A) Lamellar organization of the spicules. The almost uniformly thick layers, 4–7  $\mu\text{m}$ , form concentric cylinders. No proteinaceous material can be identified between the layers. Stepwise dissolution of the siliceous matrix: (B) After an 1 h exposure to HF, the decomposition of the silica cylinders starts. The surfaces of the lamellae become wrinkled. The dimension/thickness of one lamella (la) is indicated with the double arrowhead. After a prolonged exposure for 2 h (C and D) or 5 h (E) the solid silica material progressively disappears under the release of the proteinaceous scaffold; individual lamellae (la) are indicated (double arrowhead). The released sheets comprise holes (h). (F) Higher magnification resolves that the holes are framed by thicker spheres. (G) If the dissolution process was performed under strict avoidance of shear forces a complete proteinaceous scaffold of a lamella can be obtained.

(Fig. 2E). These scaffolds display organized structural pattern/sheets (Fig. 2F). The curtain-like sheets comprise holes with a diameter of approximately 100 nm. The rims of the holes are reinforced with thicker spheres. If the dissolution process was performed under strict avoidance of shear forces, complete proteinaceous scaffolds of lamellae can be set free (Fig. 2G). This latter result was taken as a first strong indication that the proteinaceous material within an individual lamella builds an organized web.

#### *NaDodSO<sub>4</sub>-PAGE, Western blot*

As further proof for the existence of a protein within the silica material, individual lamellae were prepared. To make it even more sure that no “contaminating” material, assumed to exist on the surface of the lamellae [36], has been included in the samples, the individual lamellae were treated again with sulfuric/nitric acid. Subsequently, the lamellae were transferred to HF to completely dissolve the inorganic silica. The remaining organic material was size-fractionated by NaDodSO<sub>4</sub>-PAGE and stained with Coomassie brilliant blue. The stained gel showed only one protein band of a size of 27 kDa (Fig. 3A, lane a). Both on the top of the gel and within the sample gel, no protein band can be visualized. In order to confirm the previously collected/documentated evidence that this 27-kDa protein cross-reacts with antibodies raised against silicatein, Western blot analysis was performed. Using this procedure, it could be shown that this 27-kDa band is recognized by the antibody preparation (Fig. 3B, lane a). In a parallel experiment, it was clarified that this antibody reaction is specific, since a preparation that had been adsorbed with recombinant silicatein from *S. domuncula* did not show any reaction (data not given).

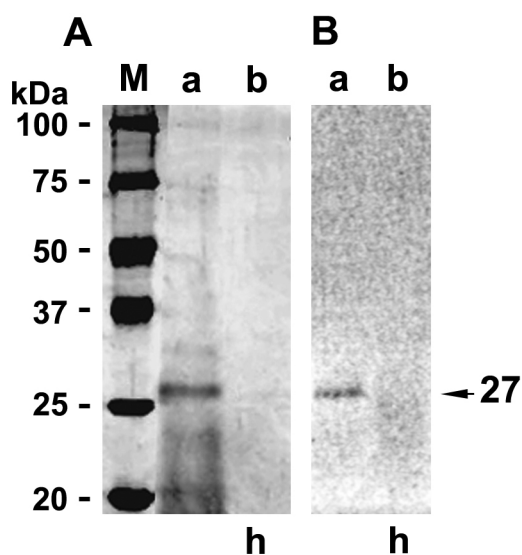


**Fig. 3** Identification of the protein existing in the lamellae of spicules from *M. chuni*. Lamellae we obtained by mechanical disintegration of the outer 1 mm of the spicules. (A) The individual lamellae were treated with sulfuric/nitric acid to remove potentially existing organic residues. Subsequently, the lamellae were exposed to HF to completely dissolve the silica material. The remaining protein was collected and subjected to 10 % NaDodSO<sub>4</sub>-PAGE, as described under “Materials and methods”. A protein sample from non-heat-treated lamellae (lane a) and from heat-treated lamellae (h), 600 °C for 20 min (extraction by equi-weight ratio), (lane b) were size separated. The gel was stained with Coomassie brilliant blue. (B) Corresponding Western blot. After size separation and transfer, the blot was reacted with polyclonal antibodies raised against silicatein. In lane a, in non-heat-treated lamellae, the single 27-kDa protein becomes brightly stained after incubation with the labeled secondary antibody preparation. In the extract from heat-treated lamellae (h), no antigen–antibody complexes can be identified.

### SEM/EDX analysis

EDX analysis is a powerful technique for the study of organic components existing in surface regions of a given substratum. An energy of 10 kV (30 s) was selected which will also ensure the analysis of the material beneath the surface. The SEM analysis (Fig. 4A) shows the piling of the silica lamellae. If the EDX analysis is performed on samples from the surface of the lamellae high levels of silicon (Si) and oxygen (O) can be measured, with over 98 wt %, while carbon (C) contributes to less than 2 wt % (Fig. 4C).

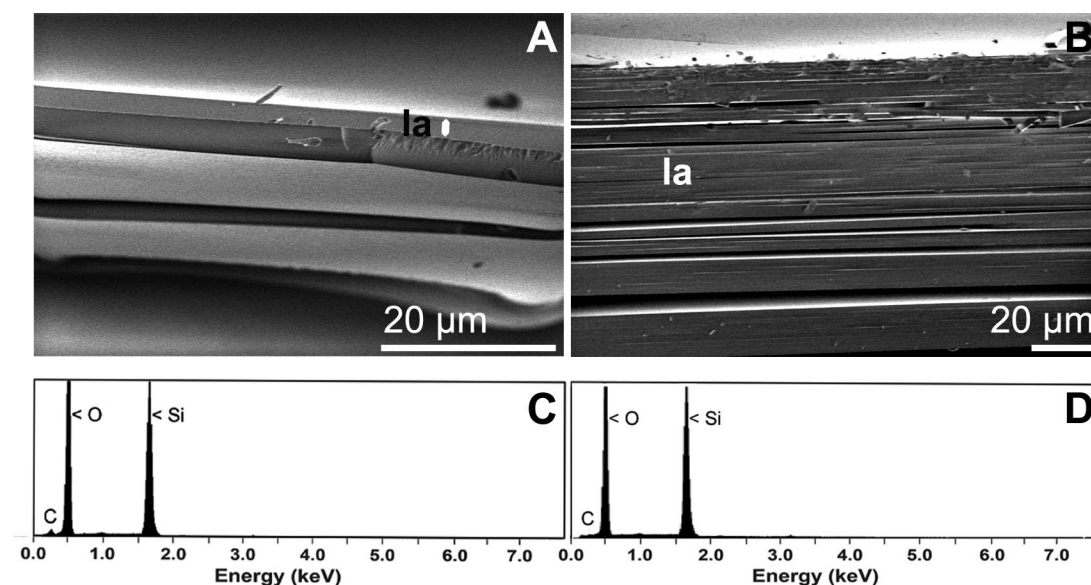


**Fig. 4** EDX analyses of the surface of lamellae from spicules. SEM image of non-heat-treated lamellae (la; and “double arrowhead”) (A); and of heat-treated lamellae (600 °C for 20 min) (B). (C) EDX determination of a surface from a non-heat-treated lamella. The dominant signals from oxygen (O) and silicon (Si) are marked. Only trace amounts of carbon (C) can be detected. (D) EDX spectrum from the surface of lamellae that had been treated at 600 °C for 20 min. Here, no signals for carbon can be identified.

### Fourier transform infrared emission spectroscopy

FT-IR spectroscopy has been performed with native and heat-treated *Monorhaphis* samples. The IR spectrum of the native *Monorhaphis* spicule (Fig. 5, red line) shows the characteristic pattern for the vibrational mode of silica (500–1300  $\text{cm}^{-1}$  range) [13]. The peaks in the spectrum can be explained as follows: the symmetric stretching signals originate from the bending of the Si–O–Si linkages (795.7  $\text{cm}^{-1}$ ); and the asymmetric stretching (1200  $\text{cm}^{-1}$ ) reflects likewise the Si–O–Si groups. Smooth bands in the 1600–2200  $\text{cm}^{-1}$  range are due to silica modes. In addition, the peak that is present at 1637.0 shows a characteristic pattern for amide (peptide) bonds, due to the presence of organic matter, e.g., proteins. This mode is in the region of C=O stretching of peptide bonds and forms the “amide I bands” [35]. The signals within the 2400–3700  $\text{cm}^{-1}$  range can be attributed to the hydroxyl (–OH) stretching and vibration modes which are due to the silanol groups on the spicule surface and to the existence of hydrogen bonds that are present in organic material. This broad range also includes modes for amine groups (–NH<sub>2</sub>), which is confirmed by the peak found at 2300  $\text{cm}^{-1}$ .

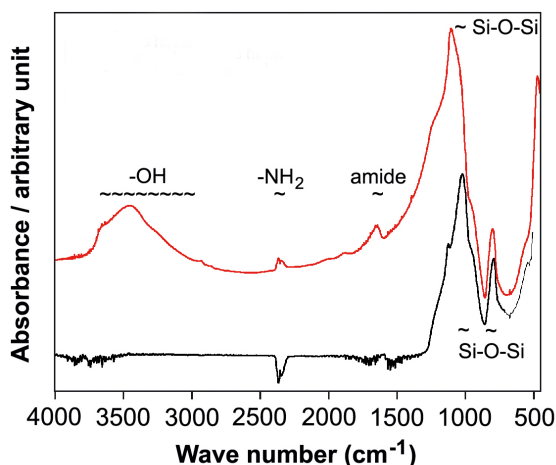


**Fig. 5** FT-IR analysis of *Monorhaphis* spicule samples, non-treated (red; upper curve) or heat-treated (600 °C; 20 min; lower curve), were analyzed within the 450–4000 wavenumber  $\text{cm}^{-1}$  range. Spectra have been recorded as described under “Materials and methods”.

#### Heat-treatment of lamellae of *M. chuni*

In this series of experiments the lamellae were treated by heat to elucidate whether the protein(s) existing there can be eliminated.

##### *Electron microscopic analysis (SEM)*

Lamellae were treated at 600 °C for 20 min in a tube oven. After this process the spicules were analyzed by SEM. The images (Fig. 6) show that no defects in the lamellar structures were caused. The giant basal spicule had been sectioned along its longer axis and one half was analyzed by SEM; it is apparent that the concentrically arranged sheets/lamellae open up and unfold (Fig. 6A). The different lamellae, constructing the spicules remained separated (Fig. 6B).

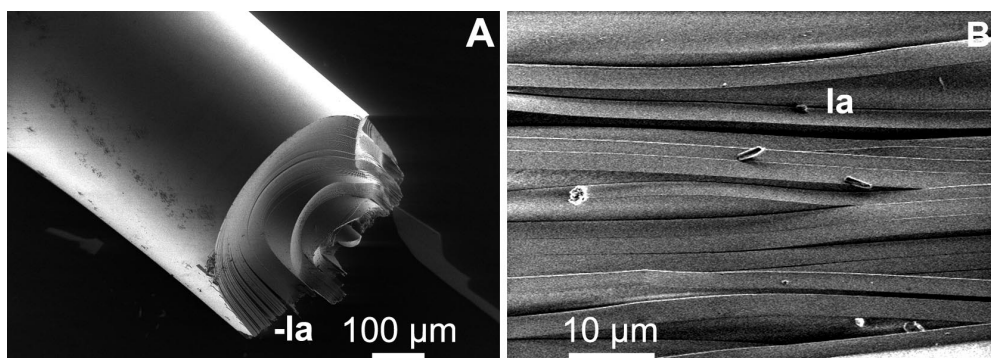


**Fig. 6** SEM analysis of giant basal spicule, after treatment at 600 °C for 20 min. (A) Overview on the spicule, after cutting along the longer axis. The organization into different lamellae, as existing in the nontreated sample, can be resolved. (B) Higher magnification of the lamellar arrangement of the spicule.

#### *NaDodSO<sub>4</sub>-PAGE, Western blot*

After heat-treatment the lamellae were extracted at an equi-weight ratio, with respect to the extraction of non-heat-treated specimens, with Tris-HCl buffer. The resulting materials were size-separated by NaDodSO<sub>4</sub>-PAGE. As seen in Fig. 3A (lane b) no protein band could be resolved. Likewise, no other band could be visualized by Coomassie brilliant blue staining. Finally, no band (antigen–antibody complex) could be identified by Western blot analysis (Fig. 3B; lane b).

#### *SEM/EDX analysis*

The heat-treated lamellae (600 °C for 20 min) from spicules show the same architecture as the non-treated lamellae (Fig. 4B). In contrast to the EDX spectrum from non-heat-treated material, that of heat-treated lamellae did not contain a measurable peak corresponding to carbon (Fig. 4D).

#### *FT-IR emission spectroscopy*

In contrast to the spectrum from non-treated lamellae, the FT-IR spectrum from lamellae that had been treated at 600 °C showed a series of distinct differences (Fig. 5, black line). Striking is the reduction of the broad peak found in the 2400–3700 cm<sup>-1</sup> range in the heat-treated sample. Likewise surprising is the disappearance of the amine group signals in the 2300 cm<sup>-1</sup> range. Also there, heat modifies the Si–O surface of the spicules, as can be deduced from the complete absence of –OH group signals from silanols in the spectra. This fact is very likely due to a process called dehydroxylation [30]. However, the remaining peaks are coincident with the characteristic pattern for the different vibrational modes of inorganic silica structure constitutive of the spicule [13].

#### *Iridium-strip heater system*

Disintegration of the lamellar structure within the giant basal spicules occurred after treatment at 1600 °C. Spicule samples were placed onto an Ir strip for increasing periods of time. Nontreated spicules show the characteristic 4–7-μm-thick lamellar organization (Fig. 7A). Based on earlier descriptions [20] a distinct zonation can be distinguished with the axial canal (diameter: ≈1 μm) in the center and the surrounding 100–150-μm-large axial cylinder of electron-dense homogeneous silica. This structure is encased by up to 400 lamellae within the lamellar region. This distinct lamellar organization is destroyed if the spicules are heated (in the lateral orientation) at 1600 °C (Fig. 7B). The lamellae fuse if the heating period exceeds 30 s (Fig. 7B). At a shorter heating period (5 s), a cracking of the lamellae is seen (Fig. 7C), while at the intermediate period of time (10–30 s) a disintegration of the lamellae occurs under simultaneous appearance of a nonstructured, foamed-up molten mass at that side which had been exposed to the heat. With increasing time, this mass increases in volume while the lamellar zone shrinks (Figs. 7E,F).

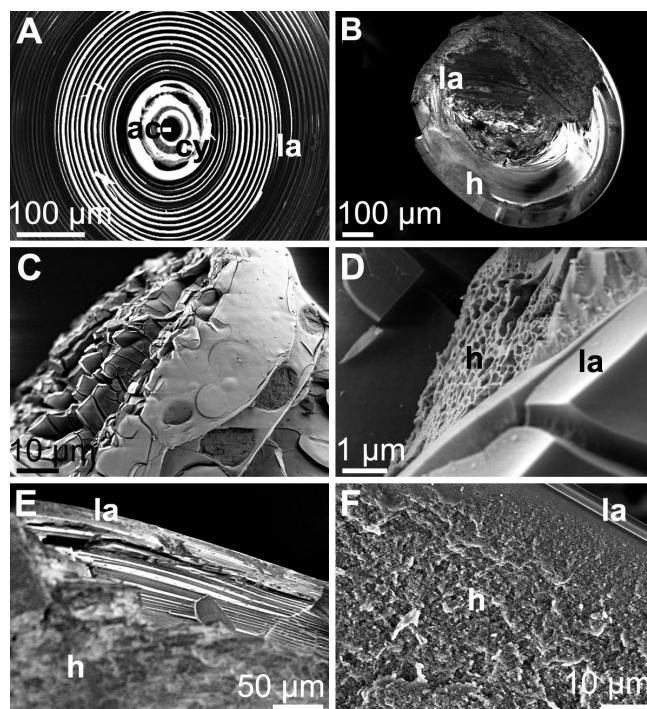


**Fig. 7** SEM analyses of *Monorhaphis* spicules that had been treated on an Ir-strip heater at 1600 °C. **(A)** Cross-section through a *Monorhaphis* giant basal spicule, showing its three parts: the axial canal (ac), in which the axial filament is located, the axial cylinder (cy) formed by dense homogeneous silica, and the main part of the spicule (lamellar region) with the regularly arranged concentric silica lamellae (la). **(B)** Giant basal spicule that had been placed onto the Ir-strip heater (1600 °C; 30 s); cross-section. The lamellae at that side which had the contact to the heating plate melted together (h), while in the opposite region lamellae (la) can still be distinguished. **(C)** Longitudinal aspect of a spicule showing the lamellae, that are spalling off (exposure: 1600 °C; 5 s). **(D)** Surface region of a heat-averted side of a spicule, showing intact lamellae (la) (breakage). In the heat-exposed opposite side (h) the lamellae are disintegrated and are replaced by a nonstructured, foamed-up molten mass (1600 °C; 10 s). Extension of the heat treatment resulted in an increase of the region displaying this molten mass (**E**; 10 s and **F**; 20 s). The two regions; heat-exposed (h) and lamellar region (la) are marked.

### Formation of silica drops in acetylene flame

In view of the recent finding that the spicules from *M. chuni* comprise up to 99.2 % of their inorganic material as Si and O, it can be concluded that the polysilicate of *Monorhaphis* has the quality of quartz glass [36]. To elucidate if glass sponge silica has the property to form glass beads, the entire skeleton of an *E. aspergillum* specimen was treated with an acetylene flame burner. The flame with a temperature of 2700 °C was directed toward the foot, the anchor-like basalia with which the animals are attached to the substratum (Fig. 8A). Already after 1 min of exposure the spicules turn to bright red and the spicules fuse (Fig. 8B). In the subsequent 5 min, the spicules form glass beads (Figs. 8C–E). Very fast, within 1–2 min after removal of the heat, the beads cool and solidify (Fig. 8F).

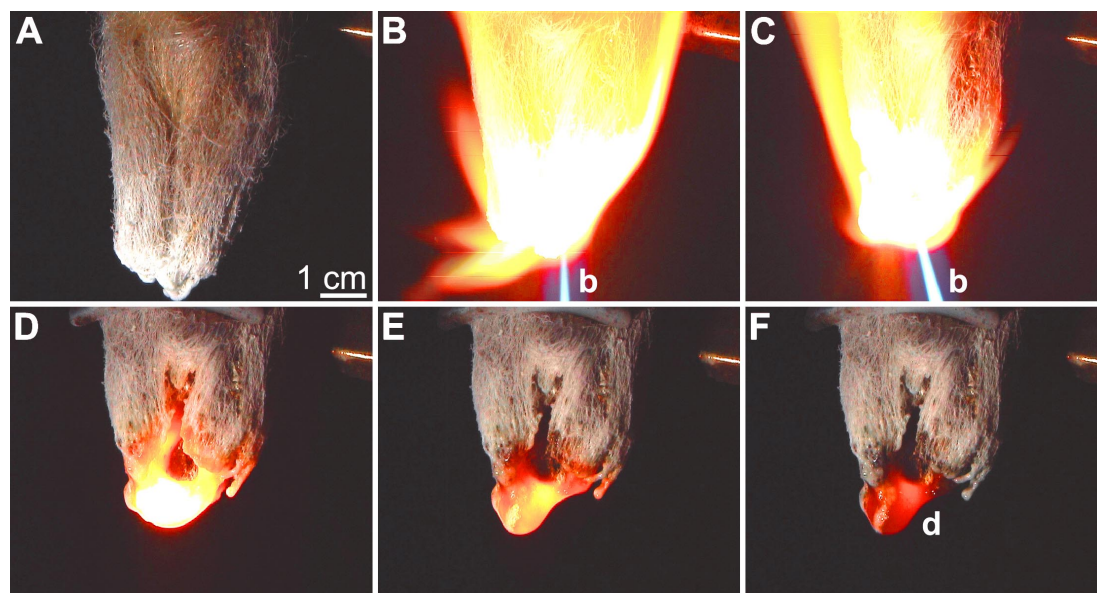


**Fig. 8** Melting of the siliceous skeleton from the hexactinellid sponge *E. aspergillum*. The skeleton was treated with a burner (b) releasing an acetylene flame which caused a temperature of about 2700 °C and mediates drop (d) formation. (A) Basis of the skeleton. Exposure to the heat for 3 min (B), 4 min (C), removal of the heat for 5 s (D), 6 s (E), and 8 s (F).

### Mechanical properties of the spicules: Flexural properties

The measurement for the flexural properties of an individual giant basal spicule of a length between 30 and 35 mm was performed in the three-point bend assay system. Spicule samples [2.1–2.6 mm (diameter)] were bent with a cross-head rate of 0.2 mm/min. The representative load-displacement curve recorded with untreated spicules showed the characteristic sequential breaking pattern [36,37]. Due to the lamellar organization of the spicules, the surface lamellae break first, a process which requires 230 N (point B). It is typical that the deflection B–C does not drop to zero. Following the viscoelastic view [38] the more central lamellae do not burst and cause resistance. In the following consecutive time interval, the subjacent lamellae break and the displacement curve reaches a value of 145 N (at D). Usually, a third flexural stress peak is reached at 128 N which has to be attributed to the inner layers of the lamellar region of the spicules (at F). Finally, the lamellae of the axial cylinder break, which displays no distinct linear/peak fracture curve [29]; the resistance of the lamellae is much lower in that region and simulates a flexible displacement (at H); Fig. 9 (red line).

Very much in contrast is the cross-head displacement record obtained with heat-treated spicules (600 °C); Fig. 9 (recording in black). The initial resistance of the spicules is much higher in comparison with the non-treated controls. A force of 365 N is needed to break the spicule (at B'), when the heat-treated spicule undergoes an almost complete breakage. A deflection B'–C' occurs which is only slightly retarded at 30 N (C'–D'), and followed by a final resistance at 5–0 N (E'–F'). These data demonstrate that the heat-treated spicules have lost the characteristic properties of the natural spicules, to comprise stiffness, flexibility, and toughness.

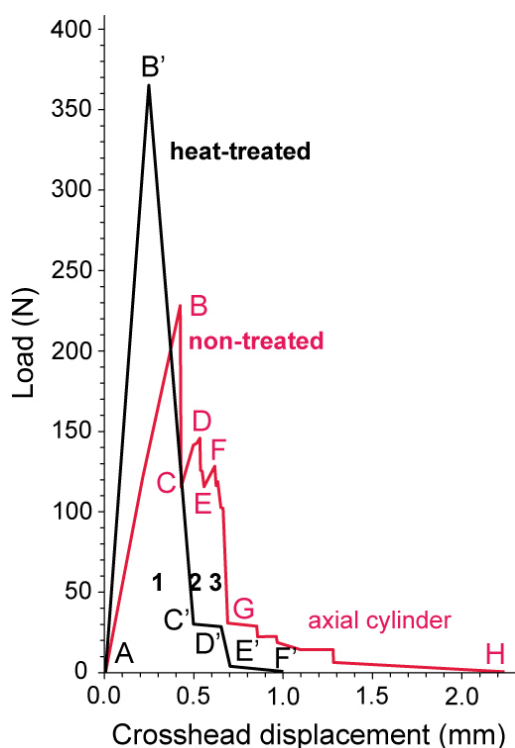


**Fig. 9** Force–displacement relationship of giant basal spicules, measured in a 3-point bending assay. Records from two representative experiments with nontreated (red curve; lower graph) and heat-treated (600 °C; 20 min, black curve) spicules are shown. In the nontreated sample, the first cracking event is recorded and is reflected by the linear increase A-B (termed “elastic response”). The first crack [1] (B) occurs and is followed by the deflection to C. Two additional breakage events [2,3] (2: C-D-E; and 3: E-F-G) are recorded before a random cracking of the different lamellae within the axial cylinder occurs. The final breakage (G-H) can be ascribed to the flexible fracture of the axial filament. In contrast, the heat-treated spicule shows in the bend test only one dominant cracking event (A-B') which is followed by minor fractures (C'-D'; E'-F').

To extend our previous SEM studies on the breaking, and chipping off of the outermost lamellae during bending in the three-point bend assay system [29], using *Monorhaphis* giant basal spicules, we have used here giant spicules from *H. sieboldi* to record in a traction device, and in a dynamic manner, the spalling of the respective outer lamellae. The spicules were subjected to a circular tension in order to record their step-wise breakage (Fig. 10). During continuous pulling/traction, the outer lamellae of the spicule did not spall off, even after having completely bent the spicule by one circumvolution (Fig. 10A). However, if the diameter of the circular torsion of the wrapped around spicule decreases below 4 cm, the first set of the outer lamellae blasts off (Fig. 10B). Then another period of flexible bending proceeds until the second breakage point is reached (Fig. 10F). Again, a further flexible bending phase takes place until a third spalling of the lamellae occurs, followed by a final fracture of the spicule (Fig. 10K).

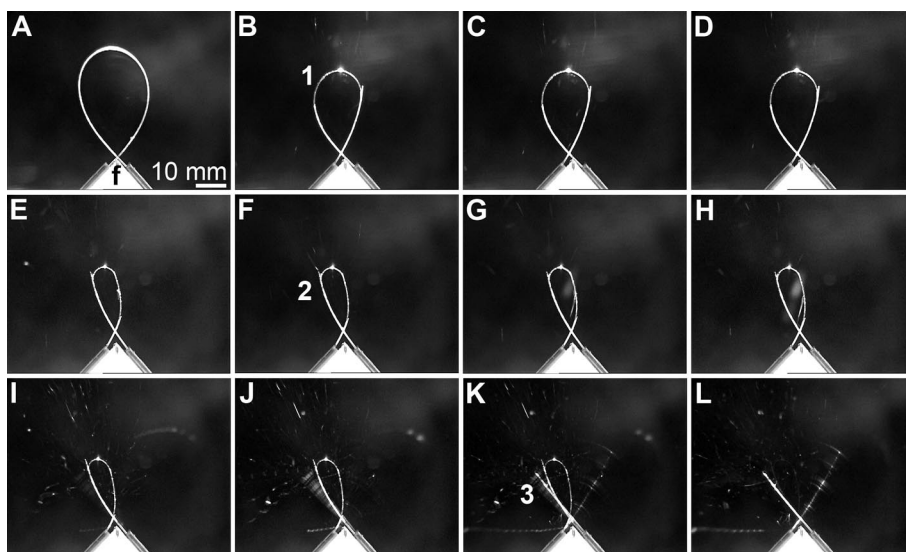


**Fig. 10** Flexible breakage of a giant spicule from *H. sieboldi*. The spicule had been inserted into a traction device between two moving rubber wheels. These continuously pulled the spicules toward the fixation point (f) using a motor. The breakage had been recorded with a high-speed camera. (A–L) Flexible and step-wise breakage of a sponge spicule. The spicule had been completely bent by one circumvolution; the diameter of the circular, wrapped around spicule was initially 4.5 cm. After proceeding traction, three step-wise breaking points can be recorded (B, F, and K) which are interrupted by phases of flexible bending.

## DISCUSSION

Using mollusk shell structures and sponge spicules as model systems, the basis for the understanding of the mechanical stability of rigid biological systems has been outlined by Mayer [1]. One key principle providing those materials with strength, stiffness, and toughness has been attributed to the presence of organic polymers within inorganic matrices. While it is well documented that in mollusk shells the organic/proteinaceous layers surround the  $\text{CaCO}_3$  platelets [1,39], the location of the protein(s) within the sponge spicules is under discussion. Since Levi [40], the giant basal spicules from the hexactinellid *Monorhaphis* gained great interest because of their remarkable property to combine toughness with stiffness and resilience. Later, the lamellar morphology of these spicules was studied with advanced electron microscopical methods [20,21]. Even though HR-SEM analyses had been performed, no protein stratum could be identified between the silica layers [29]. The view that a proteinaceous sheet exists between the silica layers, as initially reported in 1904 [37] could not be substantiated, neither in demosponges [18] nor in hexactinellids [20]. Recently, it had been demonstrated that a protein lattice exists within the inorganic matrix [22]. Published studies, claiming a different localization of the protein within the spicules, meaning that proteinaceous components (collagen) exist between individual lamellae [26], require biochemical substantiation.

While in the earlier study, the protein components within the spicules have been identified as silicatein, based on immuno-biochemical studies [22], Ehrlich [34,35] suggested that the organic material was collagen. The data given by the latter group are restricted to amino acid analyses of protein(s), extracted for 14 days with 2.5 M NaOH solution at 37 °C, from spicules of glass sponges, e.g., *Hyalonema sieboldi* [25] and *Monorhaphis* [41]. It is well established [42], and also applicable here, that under those conditions protein hydrolysis may occur. The determined high glycine content alone found in those extracts [25,41] is surely not indicative enough for the existence of collagen. The additionally mentioned results from Edman degradation [25] or NaDodSO<sub>4</sub>-PAGE [35] which remained unpub-

lished will surely not help to substantiate that view. It should be also considered that only about 30 terminal residues will be identified by Edman degradation which usually do not contain the characteristic amino acid triplet Gly-X-X [43].

In the presented study we have used, in contrast, a gentle HF extraction procedure, which might cause some post-translation modifications, e.g., phosphorylations, at the most [42]. However, besides these post-translational modifications, no protein degradation could be determined. In addition, for the extraction of protein lamellae from cleaned spicules have been used, avoiding any contamination with collagen fibrils that might have existed in the cast of the spicules. This approach unambiguously showed that it is silicatein which is detected in the inorganic matrix. This conclusion is supported also by a recent finding that demonstrates also the existence of the silicatein gene in hexactinellids [23].

Applying the same harsh extraction conditions (2.5 M NaOH, 14 days, 37 °C), structures have been visualized by SEM images, suggesting that dendritic collagen fibrils might exist between the individual lamellae [41]. However, no controls (nontreated lamellae) have yet been presented. In our SEM images it is obvious that any sign of protein layers at the surface of the lamellae is missing. However, after mild HF exposure, the proteinaceous scaffold is progressively released which has the dimensions, both in size and form, of an individual lamella.

It has been argued that it is collagen that mediates silicification [41]. However, details, e.g., concentration of the silane in the enzyme assay and documentation of analytical results, await to be presented. It should be stressed here that the characteristic feature of the silicatein reaction is that the enzymatic reaction proceeds at lower silicate-monomer concentrations, e.g., 60  $\mu$ M [10].

In the studies, presented here, the element composition of the lamellae has been determined by EDX. Besides silicon and oxygen, only minute concentrations of carbon (<2 %) have been detected on the surfaces of the lamellae, suggesting also a likewise minor presence of protein at the surface or the subjacent region. Basically, this finding is in agreement with the published data [44], which report on the presence of carbon and nitrogen besides silicon and oxygen on surfaces of spicules from hexactinellids. It is established that by variation of the primary energy and incline the surface sensitivity of the EDX technique is prone to mis-measurements [45]. However, in our determinations we have used an acceleration voltage of 10 kV and plain surfaces to avoid those interferences.

From our data, we deduce that there is no reason to assume that protein fibrils or other proteinaceous material exist on the lamellae of the spicules, but it is found within those structural units. In order to build on the recently gathered intriguing data on the unusually high fracture resistance of the giant basal spicules from *Monorhaphis* [44], it was asked if the protein lattice within the composite structure plays a crucial role in the mechanical stability. These authors already speculated that this property is largely to be attributed to the spicule architecture, meaning the alternating concentric rings of hydrated silica with its proteinaceous material [44]. At present, the most direct feasible way to resolve this question is to denature the protein in the spicules by heat as described already in 1928 [46]. This treatment will result in the destruction of the polymeric, fractal-like assemblies of silicatein (to be published), the denaturation of the primary and secondary structure of the protein and—at intensified conditions—also in removal of the protein from the spicules.

After laying a giant basal spicule from *Monorhaphis* onto an Ir-strip heater system (1600 °C), the distinct lamellar organization of the giant basal spicule is lost and the lamellae fuse. Prior to this process, the lamellae crack and the fragments undergo transformation into a foamed, molten mass that proceeds to fused glass material that does not contain any “honeycombs” and appears again crystal clear. The subsequent formation of glass drops after prolonged heat exposure was studied using the hexactinellid *E. aspergillum*. This specimen with its circular and longitudinal skeletal guide beam (diameter of around 1 mm) readily melted at a temperature of 2700 °C under formation of glass beads. Interestingly, during this drop formation it was not possible to melt together sponge bioglass with man-made amorphous glass (fused quartz) produced from silica under high temperature, even after addition of increasing concentrations of sodium carbonate (to be published). This property cannot yet be ex-

plained, since the sponge bioglass contains besides amorphous fused quartz only the most minute ingredients, e.g., sodium [36].

During heat exposure (600 °C), the protein component of the lamellae is cleared, as determined by NaDodSO<sub>4</sub>-PAGE. Not even traces of protein (27 kDa) could be identified by the Western blot technique. To confirm this conclusion, EDX analyses have been performed from the surface of the lamellae, which likewise showed that carbon, which is present in the native lamellae in low portions, is completely absent in heat-treated samples. Finally, we analyzed the lamellae prior and after heat exposure by FT-IR spectroscopy. The results show that after heat treatment the characteristic bonds, reflecting the amine groups, -OH groups, and silanols are absent. These data indicate that after heat treatment (≥600 °C) the protein component of the spicule is lost and the silica lamellae are fused together. Even though FT-IR spectroscopy has been demonstrated to be one of the most powerful methods for material characterization, it is occasionally limited, especially for materials with weak infrared absorption [47]. However, for the detection of protein within an inorganic component this technique appears to be suited.

In the final part of the study, the mechanical stability of the nontreated and the heat-treated was investigated. Previously, the characteristic property of the natural spicules, to unfold stiffness, flexibility, and toughness, has been outlined in detail [22,30]. These spicules break sequentially always averted by the intactness of the subjacent lamellae. Only during the last burst, that comprises only 15 % of the total resistance of the spicules, a flexible displacement process without resistance is recorded, which might be due to the different protein composition of the axial cylinder [22]. In contrast, the heat-treated spicules show a load-displacement curve which displays only one energy dissipation peak. The level reached exceeds that seen for the first break point of nontreated spicules by 50 %, however, on expense of the combined properties stiffness with flexibility. Following the introduced nomenclature [1], the normal spicules show a load-displacement curve which is characteristic for segmented composites, whereas heat-treated spicules break like composites with continuous layers. Using a giant spicule from *H. sieboldi* the stepwise breakage of the respective surface lamellae has been recorded by a high-speed camera. These sequences show impressively the step-wise breakage of the spicule, interrupted by periods of flexible bending.

## CONCLUSION

In conclusion, the data summarized here provide comprehensive evidence that the giant basal spicules of *Monorhaphis*, very likely to be extrapolated also to spicules from other hexactinellid species, are composed of lamellae which contain within their siliceous matrix a proteinaceous scaffold and not—as previously assumed—a protein layer between the individual lamellae. Hence, the composition of the spicules can be characterized as a genuine protein-enforced glass lamellar composite. The only (or major) component of the proteinaceous and fortifying scaffold is the spicule-synthesizing enzyme silicatein. Since the silicatein molecules from demosponges [48] and hexactinellids (to be published) form oligo- and polymers, the tear and breaking strength of the native spicules is attributed to lamellar protein/glass hybrid lamellae. Those fibers are formed—in contrast to the man-made glass hybrid composites—in nature at ambient temperature, below 30 °C. Hence, based on the results given here we expect for the future the development of biotechnological approaches allowing the fabrication of organic/inorganic (silica) hybrid fibers, suitable, for example, to build biosensors that are combined with a optofiber/waveguide connector.

## ACKNOWLEDGMENTS

We thank the Marine Biological Museum of Chinese Academy of Sciences (Qingdao) for providing us with sponge samples. Furthermore, we thank Mr. G. Glasser and Ms. M. Müller (Research group “Surface Chemistry” Dr. I. Lieberwirth and Dr. M. Kappl; Max Planck Institute for Polymer Research;

Mainz) for excellent assistance in electron microscopic analysis. We acknowledge Emily S. Damstra (Kitchener, Ontario) for providing the drawing of *M. chuni*; it is used by permission. This work was supported by grants from the European Commission [Marie Curie Research Training Network (Biocapital)], the Bundesministerium für Bildung und Forschung Germany (project: Center of Excellence *BIOTECmarin*), the International S & T Cooperation Program of China (Grant No. 2008DFA00980), the National Natural Science Foundation of China (Grant No. 50402023), and the International Human Frontier Science Program.

## REFERENCES

1. G. Mayer. *Science* **310**, 1144 (2005).
2. S. V. Patwardhan, S. J. Clarson, C. C. Perry. *Chem. Commun.* **99**, 1113 (2005).
3. H. C. Schröder, X. H. Wang, W. Tremel, H. Ushijima, W. E. G. Müller. *Nat. Prod. Rep.* **25**, 455 (2008).
4. W. E. G. Müller, X. H. Wang, S. I. Belikov, W. Tremel, U. Schloßmacher, A. Natoli, D. Brandt, A. Boreiko, M. N. Tahir, I. M. Müller, H. C. Schröder. In *Handbook of Biomineralization; Vol. 1: The Biology of Biominerals Structure Formation*, E. Bäuerlein (Ed.), pp. 59–82, Wiley-VCH, Weinheim (2007).
5. H. C. Schröder, D. Brandt, U. Schloßmacher, X. H. Wang, M. N. Tahir, W. Tremel, S. I. Belikov, W. E. G. Müller. *Naturwissenschaften* **94**, 339 (2007).
6. D. E. Morse. *Trends Biotechnol.* **17**, 230 (1999).
7. K. Shimizu, J. Cha, G. D. Stucky, D. E. Morse. *Proc. Natl. Acad. Sci. USA* **95**, 6234 (1998).
8. J. N. Cha, K. Shimizu, Y. Zhou, S. C. Christianssen, B. F. Chmelka, G. D. Stucky, D. E. Morse. *Proc. Natl. Acad. Sci. USA* **96**, 361 (1999).
9. A. Krasko, R. Batel, H. C. Schröder, I. M. Müller, W. E. G. Müller. *Eur. J. Biochem.* **267**, 4878 (2000).
10. W. E. G. Müller, U. Schloßmacher, X. H. Wang, A. Boreiko, D. Brandt, S. E. Wolf, W. Tremel, H. C. Schröder. *FEBS J.* **275**, 362 (2008).
11. S. L. Walter, B. D. Flinn, G. Mayer. *Acta Mater.* **3**, 377 (2006).
12. M. J. Uriz, X. Turon, M. A. Beccero. *Progr. Mol. Subcell. Biol.* **33**, 163 (2003).
13. F. Sandford. *Microsc. Res. Technol.* **62**, 336 (2003).
14. S. P. Leys, G. O. Mackie, H. M. Reiswig. *Adv. Marine Sci.* **52**, 1 (2007).
15. H. C. Schröder, F. Natalio, I. Shukoor, W. Tremel, U. Schloßmacher, X. H. Wang, W. E. G. Müller. *J. Struct. Biol.* **159**, 325 (2007).
16. J. Aizenberg, J. C. Weaver, M. S. Thanawala, V. C. Sundar, D. E. Morse, P. Fratzl. *Science* **309**, 275 (2005).
17. W. E. G. Müller, M. Wiens, T. Adell, V. Gamulin, H. C. Schröder, I. M. Müller. *Int. Rev. Cytol.* **235**, 53 (2004).
18. W. E. G. Müller, M. Rothenberger, A. Boreiko, W. Tremel, A. Reiber, H. C. Schröder. *Cell Tissue Res.* **321**, 285 (2005).
19. C. Gröger, K. Lutz, E. Brunner. *Cell Biochem. Biophys.* **50**, 23 (2008).
20. W. E. G. Müller, C. Eckert, K. Kropf, X. H. Wang, U. Schloßmacher, C. Seckert, S. E. Wolf, W. Tremel, H. C. Schröder. *Cell Tissue Res.* **329**, 363 (2007).
21. X. H. Wang, J. Li, L. Qiao, H. C. Schröder, C. Eckert, K. Kropf, W. E. G. Müller. *Acta Zool. Sinica* **53**, 557 (2007).
22. W. E. G. Müller, A. Boreiko, U. Schloßmacher, X. H. Wang, C. Eckert, K. Kropf, J. Li, H. C. Schröder. *J. Exp. Biol.* **211**, 300 (2008).
23. W. E. G. Müller, X. H. Wang, K. Kropf, A. Boreiko, U. Schloßmacher, D. Brandt, H. C. Schröder, M. Wiens. *Cell Tissue Res.* **333**, 339 (2008).

24. H. Ehrlich, H. Worch. In *Handbook of Biomineralization, Vol. 1: The Biology of Biominerals Structure Formation*, E. Bäuerlein (Ed.), pp. 23–41, Wiley-VCH, Weinheim (2007).
25. H. Ehrlich, H. Worch. In *Porifera Research: Biodiversity, Innovation and Sustainability [Proceedings of the “7th International Sponge Symposium 2006, Buzios, Rio de Janeiro, Brasil; May 07–13, 2006”]* Série Livros 28. Museu Nacional, Rio de Janeiro. 2007, M. R. Custódio, G. Lôbo-Hajdu, E. Hajdu, G. Muricy (Eds.), pp. 303–312, Museo Nacional, Rio de Janeiro (2007).
26. K. R. Tabachnick. In *Systema Porifera: A Guide to the Classification of Sponges*, N. A. Hooper, R. W. M. v. Soest (Eds.), pp. 1264–1266, Kluwer Academic, New York (2002).
27. B. Stoll, K. P. Jochum, K. Herwig, M. Amini, M. Flanz, B. Kreuzburg, D. Kuzmin, M. Willbold, J. Enzweiler. *Geostand. Geoanal. Res.* **31**, 1 (2007).
28. U. K. Laemml. *Nature* **227**, 680 (1970).
29. W. E. G. Müller, X. H. Wang, K. Kropf, H. Ushijima, W. Geurtsen, C. Eckert, M. N. Tahir, W. Tremel, A. Boreiko, U. Schloßmacher, J. Li, H. C. Schröder. *J. Struct. Biol.* **161**, 188 (2008).
30. J. T. Klopogge, S. Komarneni, K. Yanagisawa, R. Fry, R. L. Frost. *J. Colloid Interface Sci.* **212**, 562 (1999).
31. G. Mayer, M. Sarikaya. *Exper. Mechanics* **42**, 395 (2002).
32. M. Sarikaya, H. Fong, N. Sunderland, B. D. Flinn, G. Mayer, A. Mescher, E. Gaino. *J. Mater. Res.* **16**, 1420 (2001).
33. K. Autumn, C. Majidi, R. E. Groff, A. Dittmore, R. Fearing. *J. Exp. Biol.* **209**, 3358 (2006).
34. S. Compton, C. Jones. *Anal. Biochem.* **151**, 369 (1985).
35. P. I. Haris, F. Severcan. *J. Mol. Catal., B: Enzym.* **7**, 207 (1999).
36. W. E. G. Müller, K. Jochum, B. Stoll, X. H. Wang. *Chem. Mater.* **20**, 4703 (2008).
37. F. E. Schulze. *Hexactinellida. Wissenschaftliche Ergebnisse der Deutschen Tiefsee-Expedition auf dem Dampfer “Valdivia” 1898–1899*, pp. 1–266, Gustav Fischer Verlag, Stuttgart (1904).
38. G. Mayer, R. Trejo, E. Lara-Curzio, M. Rodriguez, K. Tran, H. Song, W. H. Ma. *Mater. Res. Soc. Symp. Proc.* **844**, Y4.2.1 (2005).
39. F. Marin, B. Pokroy, G. Luquet, P. Layrolle, K. De Groot. *Biomaterials* **28**, 2368 (2007).
40. C. Levi, J. L. Barton, C. Guillemet, E. Le Bras, P. Lehuede. *J. Mater. Sci. Lett.* **8**, 337 (1989).
41. H. Ehrlich, S. Heinemann, C. Heinemann, P. Simon, W. Bazhenov, N. P. Shapkin, R. Born, K. R. Tabachnick, T. Hanke, H. Worch. *J. Nanomater.* (2008). DOI:10.1155/2008/623838
42. H. C. Schröder, A. Boreiko, M. Korzhev, M. N. Tahir, W. Tremel, C. Eckert, H. Ushijima, I. M. Müller, W. E. G. Müller. *J. Biol. Chem.* **281**, 12001 (2006).
43. R. Garrone. *Prog. Mol. Subcell. Biol.* **21**, 191 (1998).
44. H. Ehrlich, A. V. Ereskovskii, A. L. Drozdov, D. D. Krylova, T. Hanke, H. Meissner, S. Heinemann, H. Worch. *Russ. J. Marine Biol.* **32**, 186 (2006).
45. U. Scheithauer. *Fresenius’ J. Anal. Chem.* **341**, 445 (1991).
46. W. J. Schmidt. *Die Pfahlnadel von Monorhaphis chuni* F. E. Schulze. *Mikrokosmos* **21**, 113 (1928).
47. K. L. Andrew Chan, S. G. Kazarian. *Analyst* **131**, 126 (2006).
48. W. E. G. Müller, A. Boreiko, U. Schloßmacher, X. H. Wang, M. N. Tahir, W. Tremel, D. Brandt, J. A. Kaandorp, H. C. Schröder. *Biomaterials* **28**, 4501 (2007).